Proceedings of the 17th International Heat Transfer Conference, IHTC-17
14 – 18 August 2023, Cape Town, South Africa

IHTC-17 | ID: 486

VALIDATION OF HIGH-DEFINITION FIBER OPTIC SENSORS FOR TEMPERATURE AND LOCAL HEAT TRANSFER COEFFICIENT MEASUREMENTS OF SYMMETRICALLY HEATED, SINGLE-PHASE INTERNAL FLOW

Lindsey V. Randle[1*] and Brian M. Fronk[1]

[1]The Pennsylvania State University, Department of Mechanical Engineering
University Park, PA 16802, USA

ABSTRACT

The objective of this paper is to use fiber optic sensors embedded in a tube wall to measure local convective heat transfer coefficients of a single-phase fluid. By using Rayleigh backscatter and an interferometer technique, mechanical changes in a fiber sensor that are proportional to temperature can be detected. This allows the location and magnitude of the temperature along the fiber to be measured. Using these fibers, we can measure axial profiles of the wall temperature in a heated tube with an internal fluid. By using multiple sensors spaced circumferentially around the tube, we can then generate axial and circumferential temperature maps of the tube wall. When combined with a known uniformly applied heat flux, these measurements can be used to determine the local heat transfer coefficients for single-, two-phase, and supercritical flows.

In this study we consider a horizontal tube with internal diameter of 4.57 mm and heated length of 0.4 m. Using the fibers, wall temperature is measured every 0.7 mm in the streamwise direction at eight evenly spaced axial locations with an uncertainty of 2 °C. Co-located, calibrated thermocouples will verify the fiber temperature readings. Electric heaters provide a heat flux up to 20 W/cm^2. Using this setup, heat transfer coefficients in the developing and fully developed region are obtained for water in laminar flow regimes and compared with established convective heat transfer correlations and models. The measured heat transfer coefficients in agreement with what is expected. In future work, this test section will be used to study near-critical carbon dioxide convective heat transfer in both steady and transient conditions.

KEY WORDS: Measurement techniques, local convective heat transfer coefficients, distributed temperature sensor

1. INTRODUCTION AND PRIOR WORK

It is often desirable to find the local heat transfer coefficients for in-tube convective heat transfer. This is particularly true for the study of flows where the properties of the working fluid and therefore the heat transfer will vary dramatically within a small distance, for example in boiling and near/supercritical fluids. Many local temperature measurements are needed to calculate the heat transfer coefficients. Often this is achieved with thermocouples, resistance temperature detectors (RTDs), thermistors or similar point measurement tools. For example, 128 thermocouples were used to measure the local heat transfer coefficient of supercritical R134a in a circular horizontal tube in the study by Tain et. al [1]. Similar techniques have also been used in the following studies [2-4]. These approaches provide the desired measurement however, due to the high cost per device and limited capacity of data acquisition systems, the number of discrete temperature measurements is often limited. The recent development and

*Corresponding Author: randlel@psu.edu

commercialization of fiber optic sensors allows for a single fiber to measure an array of temperatures at many locations along the fiber. Thus, a single fiber can be used to replace hundreds of axially dispersed point measurement devices.

In our study, we correlate the physical change in shape of a silica glass fiber with a well characterized thermal expansion coefficient as it is heated or cooled due to thermal strain. A coherent wave laser is swept over a fixed frequency and the light is split between the test fiber and a reference path. Some light is backscattered via Rayleigh scattering from each fiber, which is combined, and a periodic interference pattern can be detected. This pattern can then be correlated to the distance of inherent scattering sites within the fiber from the source. These sites are unique to each fiber and do not change over the range of temperatures considered in this study. As the fiber is heated or cooled, it will locally expand or contract according to the coefficient of thermal expansion. Using the interferometer technique described above, the relative change in scattering site locations from the source can be calculated and then correlated to both a position along the fiber and a temperature change using the known coefficient of thermal expansion. For the commercial optical system in this study, we can obtain temperature measurements at a spatial gauge distance of 0.7 mm.

Our research group has used this temperature sensing approach to characterize the heat transfer of condensing and evaporating refrigerants [5-6]. In these studies, a horizontal copper tube containing refrigerant was heated or cooled by water flowing through an annulus surrounding the inner tube. A fiber was installed within a capillary tube immersed in the annulus at a set distance from the refrigerant tube. This allowed the axial measurement of the water temperature, which could be used to calculate the condensation/evaporation heat duty. The fiber measurement was verified with co-located RTDs, and the refrigerant tube surface temperature was measured using surface mount thermocouples. The study showed good agreement between fiber measurements and co-located RTDs, and the calculated heat transfer coefficients agreed well with established correlations. However, the heat transfer coefficients were still averaged over some distance, as local tube wall temperature was not available.

In a subsequent study, our research group sought to characterize the local inner and outer wall temperature of a heated annular channel containing flowing air using fiber optic sensor embedded within the tube wall [7]. A metal additively manufactured heat exchanger was developed that allowed the fiber sensor to be installed in a manner to measure axial and circumferential wall temperature distributions within the channel. Experiments were conducted at wall temperatures up to 500 °C and transient and steady state temperature maps generated for different operating conditions. However, local heat transfer measurements were not obtained, and the co-located thermocouples or RTDs were not available to verify the fiber measurements.

Other research groups have also used similar methods to characterize temperatures of flows and surfaces such as simulated fuel rods. The fibers are often placed directly in the flow like in the work of Lomperski et al. [8] and in our own group's prior work [6, 9]. For example, Gerardi et al. placed the fibers in liquid sodium with a supercritical carbon dioxide jet to study the interaction. Silica fibers were advantageous for this study because they are resistant to the corrosive liquid sodium environment [10]. The fibers are also being used in research for nuclear applications, Hurley and Duarte used these fibers to find the heat flux for fuel rod quenching [11].

A key limitation of our prior work and that of others is that they either did not embed fibers within tube walls or did not use the measured temperature to obtain local heat transfer coefficients. Thus, the goal of this work is to demonstrate the potential to measure local heat transfer coefficients of an internal flow using fiber sensors embedded directly within the tube wall. Multiple sensors will be spaced circumferentially around the tube to generate axial and circumferential temperature maps of the tube wall. These data can be used with a constant heat flux boundary to calculate the local heat transfer coefficients. The experiments in this study are conducted with water. In future work, this validated technique will be extended to variable property flows of near- and supercritical fluids.

2. EXPERIMENTAL APPROCH AND ANALYSIS METHODS

2.1 Test Loop We conducted experiments in an single-pressure loop, using deionized water at atmospheric pressure. A schematic of the loop is shown in Fig 1. The flow loop is a closed system that consists of a gear pump, the heated test section, and a post-cooler. The water is pumped by a magnetically coupled, variable speed micro-pump gear pump (Micropump Model GC M23). The flow rate is set manually using the measurement from the Coriolis flow meter with a nominal uncertainty of 0.1%. The post-cooler is a tube-in-tube heat exchanger with the experimental working fluid in the inner tube. The cooling load is provided by a 1.3 kW chiller. The inlet and outlet temperature of the test section are measured by T-type thermocouples calibrated to an uncertainty of ± 0.1 °C. The absolute pressure at the inlet and differential pressure across the test section are measured by a Rosemount 3051SMV pressure transducer. The pressure transducer has an uncertainty of ± 20 kPa and ± 0.2 kPa for the absolute and differential pressures respectively. Heat is added to the loop in the test section using ten 425-watt band heaters. The power input is controlled by a single-phase silicon controlled rectifier (SCR) and measured using a watt meter (Ohio Semitronics PC5-110EY25).

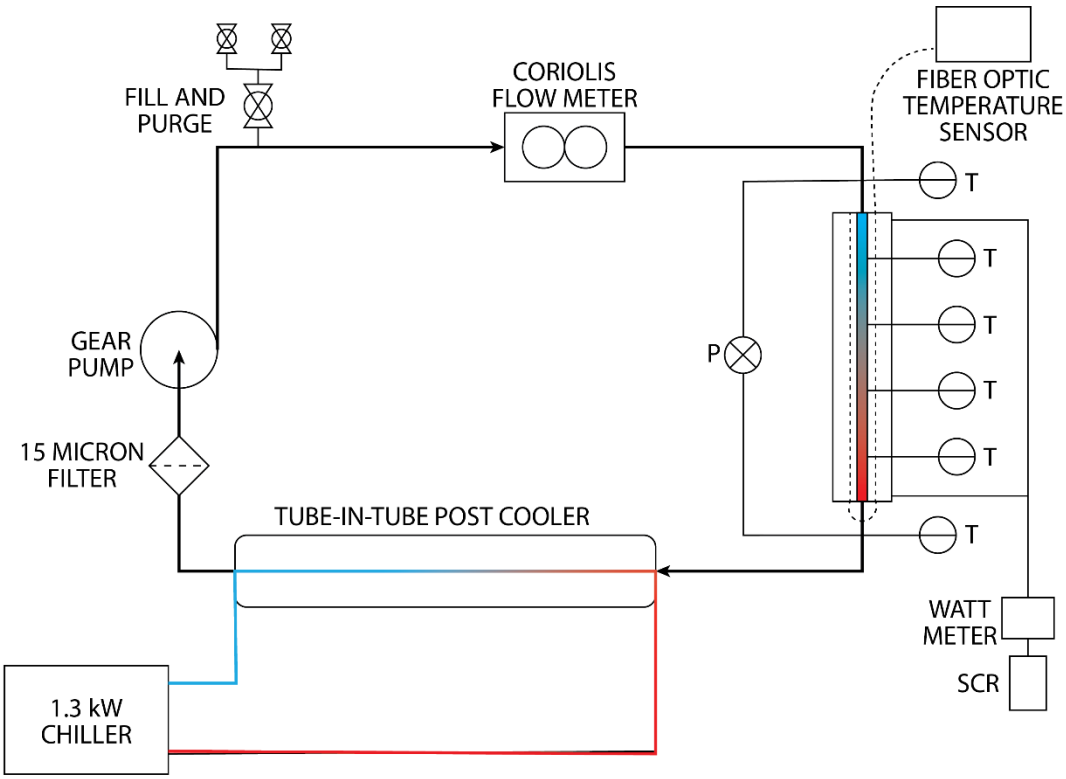

Fig. 1 Experimental Loop Schematic

2.2 Test Section The test section design utilizes fiber optic temperature measurements to capture wall temperatures along the full test section length at eight axial locations of the tube, see Figure 2. With the current system, LUNA OSiDI 6000 series interrogator, we are able obtain 20 Hz capture rates with a spatial resolution of 0.7 mm [12]. The 5 m fiber is looped back and forth through the channels along the 0.4 m heated section of the tube. We measure temperature at 617 discrete points for each of the 8 axial locations resulting in 4,936 temperature measurements.

The test section uses an aluminum sleeve between the circular, stainless steel tube and the heaters. The sleeve concentrates the lower heat flux at the outer surface from large diameter heaters to the smaller

4.75 mm inner tube diameter to achieve the high heat fluxes desired for future experiments (> 20W/m^2). A copper shim wrapped around the stainless steel tubing helps reduce contact resistance between the aluminum sleeve and the stainless tube. Because of the optical fiber's location in the aluminum block a correction is needed to better represent the inner wall temperature, see section 2.3 for this correction. Four T-type thermocouples are installed in slots in the aluminum sleeves with their probes at the same radial location as the fibers, see Figure 2B.

The full assembly is surrounded by 5 cm of mineral wool insulation (k = 0.035 W/mK). This minimizes the heat loss to the room and allows the heat into the fluid to be equal to that of the measured power into the heaters. With this thickness of insulation, the heat loss into the room is estimated to be approximately 0.3% of the total heat rate at full heater power. Therefore, we neglect this heat loss into the room.

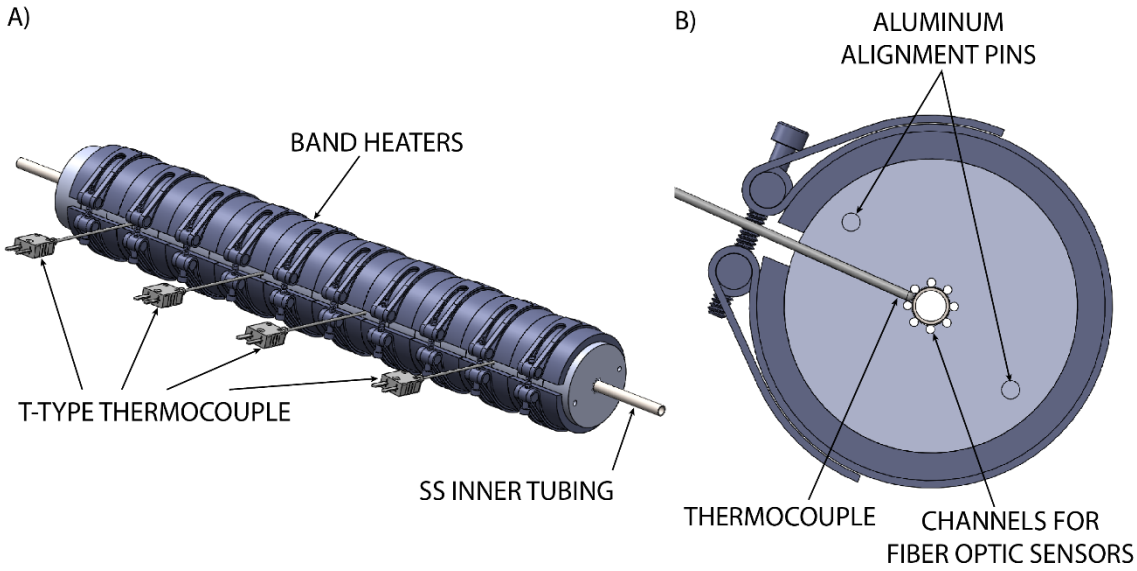

Fig. 2 Visual Representation of the Test Section A) Full View B) Cross Section

2.5 Calibration of the Fiber The calibration was performed with the fibers installed in the test section to minimize changes in mechanical strain between the calibration and data collection. The reference temperature was found using the T-type thermocouples installed in the test section that are calibrated to 0.1 °C. The water was preheated using heat tape at the inlet of the test section. All calibration data were collected at steady state with the band heaters off to allow for a uniform temperature down the length of the test section. Measurements were recorded at six temperatures from 20 °C to 60 °C. A calibration curve was found for each point along the fiber to bring those measurements into agreement with the thermocouples. This is done before any spatial averaging occurs so that every temperature measurement has a unique calibration curve. This calibration procedure was performed twice, once before and once after the experiments. The uncertainty for the calibrations were ± 2.0 °C and ± 1.0 °C respectively. For further analysis we will use ± 2 °C which is the given uncertainty from the manufacturer for the fibers. When applied to the same data, the calibrations are in good agreement as seen in Figure 3. When the band heaters in the test section are turned on there is less agreement between the thermocouples and the fibers even after the calibration is applied, we believe this is due to conduction in the metal probe of the thermocouple from the hotter sections of the heated aluminum sleeve.

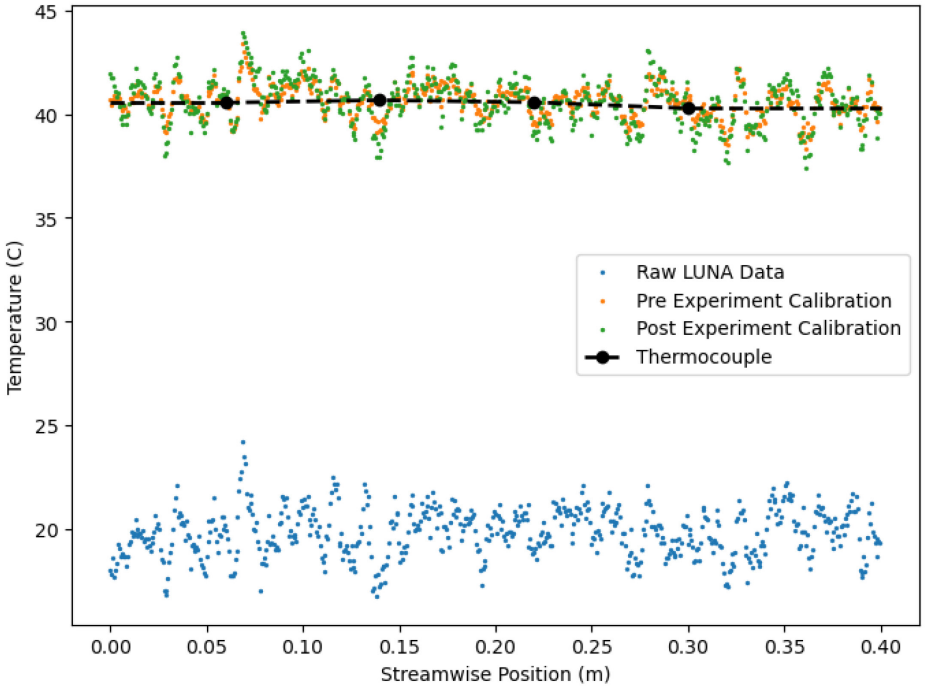

Fig. 3 Fiber Calibration Applied to Data Collected with the Test Section at a Uniform Temperature and Steady State

2.3 Heat Transfer Analysis For these experiments, we are operating at steady state conditions therefore the data from each temperature measurement location is averaged over time. The heaters provide symmetric heating around the tube and buoyancy is not expected to have a large effect on the flow so the temperatures of the eight axial temperature locations are averaged for each streamwise location. The assumption to neglect buoyancy effects was confirmed by comparing the fiber temperatures at the top and bottom of the test section. The differences between the fiber temperatures were about 3% which is comparable to the temperature differences between any two of the axial positions. However, in future work we expect the effect of buoyancy to be significant so each axial location will be considered independently. We also account for the thermal resistance of the copper and stainless steel wall between the optical fiber and the fluid. Equation 1 was used to calculate the wall temperature for each streamwise location, where T_{fiber} is the calibrated temperature measurement from the fiber optic sensor and the thermal resistances are defined in Equation 2.

$$T_{wall} = T_{fiber} - q_{node}(R_{ss} + R_{cu}) \tag{1}$$

$$R_{ss} = \frac{\ln\left(\frac{D_o}{D_i}\right)}{2\pi k_{ss} L_{node}} \text{ and } R_{cu} = \frac{\ln\left(\frac{D_o}{D_i}\right)}{2\pi k_{cu} L_{node}} \tag{2}$$

The bulk temperature is calculated using a nodal analysis. The heat flux is assumed to be constant and symmetric and is derived from the measured heat rate into the band heaters. Equation 3 is used to calculate the bulk temperature for a node (i), using the enthalpy from the previous node (i-1) and the heat rate into each node divided by the mass flow rate. The inlet temperature measured by a thermocouple in direct contact with the water is used for the inlet of the first node of the test section. The pressure is assumed to be constant along the length of the tube, this assumption is verified by the differential pressure measurement across the test section of 0.12 kPa. Once the bulk temperatures are found the local heat transfer coefficients can be calculated using Equation 4.

$$T_{bulk,i} = T(\, h_{i-1} + q_{node}/\dot{m},\ P) \tag{3}$$

$$h = q" (T_{wall} - T_{bulk}) \quad (4)$$

2.4 Uncertainty Analysis The uncertainty of the heat transfer coefficients is found by propagating the uncertainty due to the wall temperatures and heat rate using Figliola and Beasley's sequential propagation method [13]. The wall temperature measurement uncertainty is ± 2 °C for the fiber optic sensors and the heat rate uncertainty is ± 5.70 W. The wall temperature and heat flux make up the majority of the uncertainty.

3. RESULTS AND DISCUSSION

We estimate the heat transfer coefficients throughout the test section using a Nusselt number of 4.36 for fully developed laminar flow with constant heat flux. Figure 4 shows the estimated heat transfer coefficient value compared to the measured heat transfer coefficient from the fiber optic sensor. The percent difference between the predicted and measured values is at most 7.2% for the full test section. The vertical dashed line shows where the flow becomes fully developed, after this point the percent difference at most 2.7%.

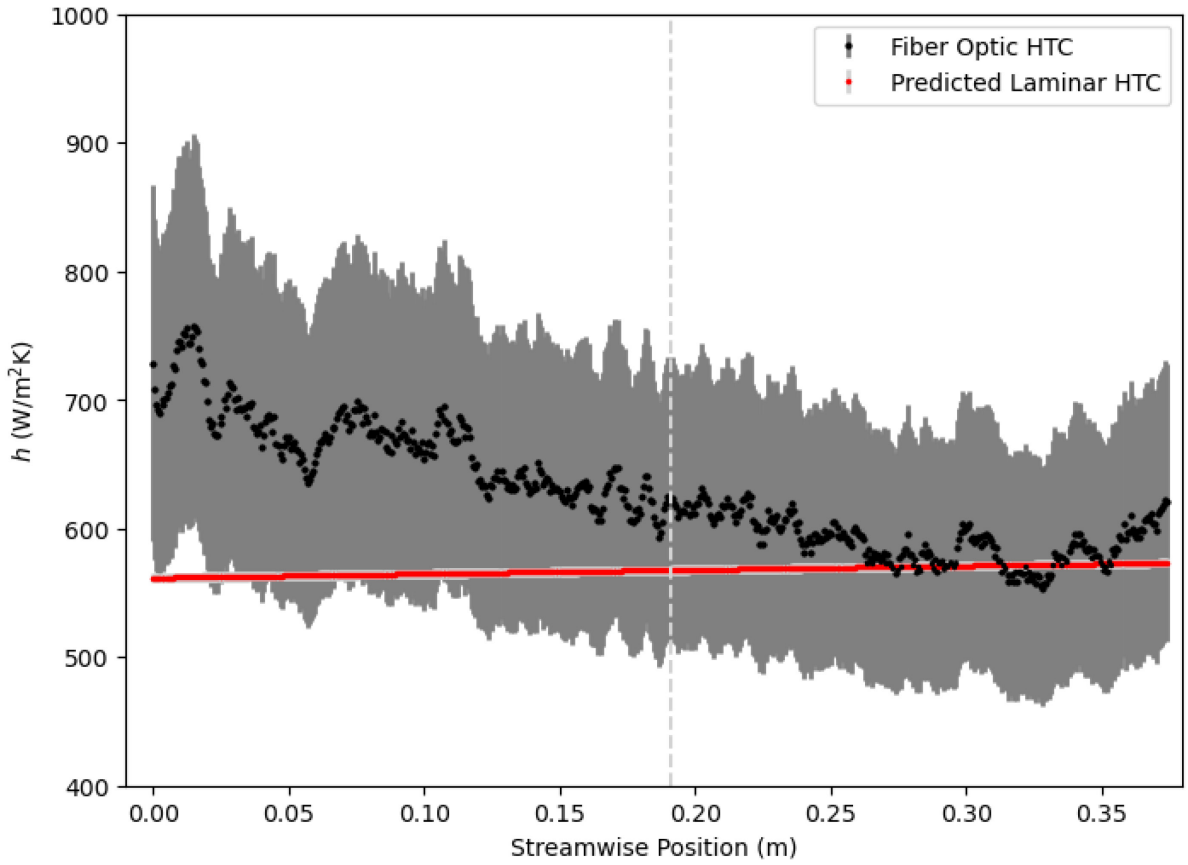

Fig. 4 Heat Transfer Coefficients for Flow of Water (Re = 5880, $q"$ = 6.58 W/cm^2)

The temperatures from the fiber optic sensors along with the bulk fluid temperatures calculated from Equation 3 are shown in Figure 5. The bulk temperature, estimated heat transfer coefficient, and heat flux are used to find an estimated wall temperature.

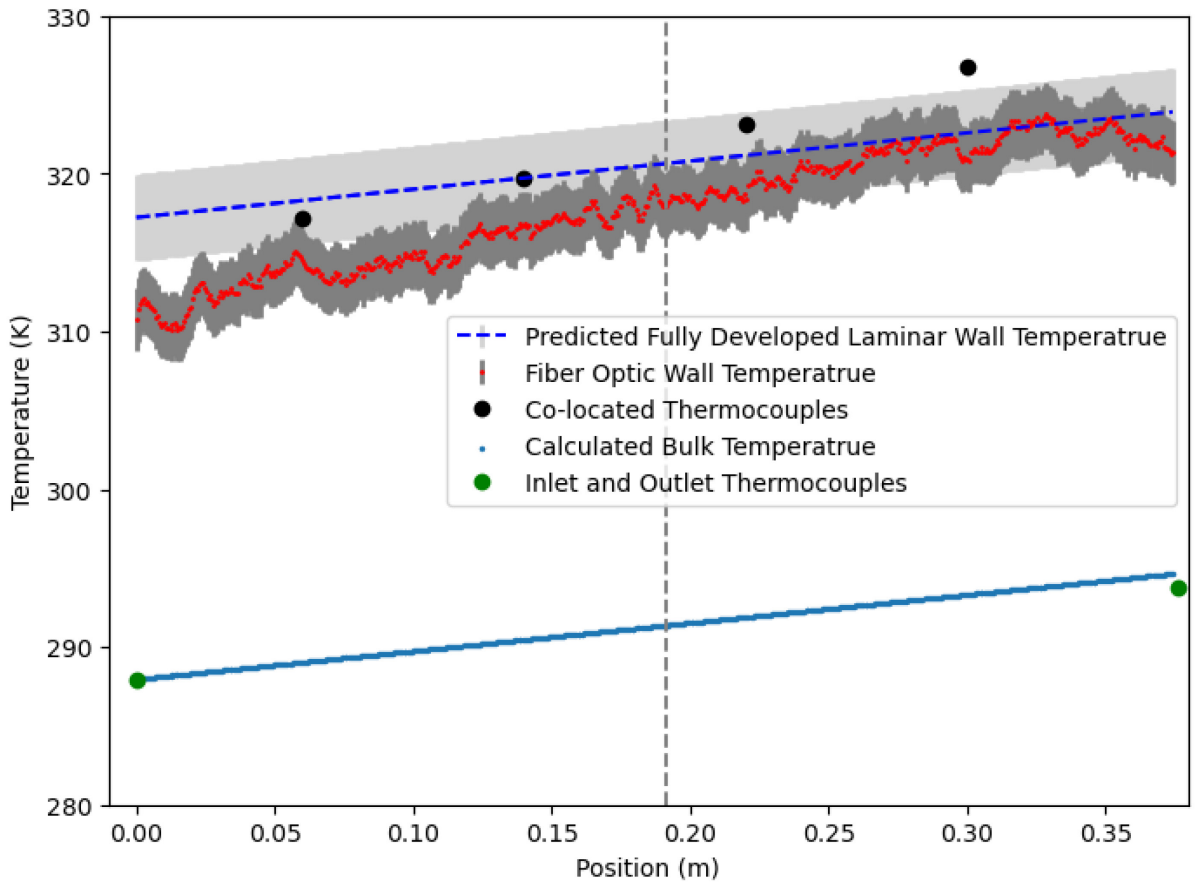

Fig. 5 Measured Wall Temperatures of Turbulent Water (Re = 5880, q'' = 6.58 W/cm^2)

The energy balance of the system was confirmed by comparing the measured power supplied to the heaters and the advective heat found using the fluid inlet and outlet temperatures. The total difference between these measurements is 12.6W with a percent difference of 15.2%. While this is larger than desired, we suspect that this may be due to conduction through the tubing connected to the test section. We have insulated the tubing around the inlet and outlet of the test section to reduce this effect for future experiments.

4. CONCLUSIONS

This work is intended to validate the use of distributed fiber optic temperature sensing in measuring local heat transfer coefficients. This data shows good agreement of the heat transfer coefficients compared to the expected value in fully developed laminar flow. However with further refinement of the fiber optic measurements, the local heat transfer coefficients could be measured more accurately and the associated error could be further reduced. In future work, we aim to use this technique to measure instabilities in supercritical carbon dioxide.

ACKNOWLEDGMENT

This material is based upon work supported by the National Science Foundation under Grant No. 1604433.

NOMENCLATURE

T_{wall}	inner tube wall temperature	[K]	$\dot{m}$	mass flow rate	[kg/s]
T_{fiber}	fiber temperature	[K]	P	pressure	[kPa]
T_{bulk}	bulk fluid temperature	[K]	q_{node}	heat into a single node	[W]
Re	Reynolds Number	[ ]	q''	heat flux	[W/m^2]
h_i	node enthalpy	[J/kg]	Nu	Nusselt Number	[ ]
h	convective heat transfer coefficient	[W/m^{2}K]			

REFERENCES

[1] Tian, R., He, S., Wei, M., and Shi, L., "The staged development of a horizontal pipe flow at supercritical pressure," *Int. J. Heat Mass Transf.*, 168 pp. 120 841, (2021). **Journal Paper**

[2] Wang, Y., Li, S., and Dong, M., "Experimental investigation on heat transfer deterioration and thermo-acoustic instability of supercritical-pressure aviation kerosene within a vertical upward circular tube," *Applied Thermal Engineering*, 157, (2019). **Journal Paper**

[3] Cai, D., Xu, X., Zhang, S., Liu, C., and Dang, C., "Experimental investigation on the flow instability of supercritical CO2 in vertical upward circular tube in trans-critical CO2 Rankine system," *Applied Thermal Engineering*, 183 pp.116-139, (2021). **Journal Paper**

[4] Xu, J., Zhang, H., Zhu, B., and Xie, J., "Critical supercritical-boiling-number to determine the onset of heat transfer deterioration for supercritical fluids," *Solar Energy*, 195 pp. 27–36, (2020). **Journal Paper**

[5] Jacob, T. A., and B. M. Fronk. "Use of Optical Distributed Sensors for Spatial Temperature Measurements in HVAC & R Research." *ASHRAE Annual Conference*, (2018). **Conference Proceedings**

[6] Jacob, T. A., Matty, E. P., and Fronk, B. M., "Use of Distributed Temperature Sensors for Condensation Heat Transfer Measurements of R-134a in Circular Channels." *ASTFE 4th Thermal and Fluids Engineering Conference*. (2019). **Conference Proceedings**

[7] Gaudin, G., and Fronk, B. M., "Distributed Temperature Measurement in an Additively Manufactured Heat Exchanger Using Embedded Fiber Optic Sensors." *19th International Topical Meeting on Nuclear Reactor Thermal Hydraulics (NURETH-19)*. (2022). **Conference Proceedings**

[8] Lomperski, S., Gerardi, C., and Pointer, W. D., "Fiber optic distributed temperature sensor mapping of a jetmixing flow field," *Experiments in Fluids*, 56(3), pp.1–16. (2015). **Journal Paper**

[9] Jacob, T. A., Matty, E. P., and Fronk, B. M., "Experimental investigation of in-tube condensation of low GWP refrigerant R450A using a fiber optic distributed temperature sensor." *Int. J. of Refrigeration* (103), (2019). **Journal Paper**

[10] Gerardi, C., Bremer, N., Lisowski, D., Lomperski, S., "Distributed temperature sensor testing in liquid sodium." *Nuclear Engineering and Design*, 312, pp. 59-65 (2017). **Journal Paper**

[11] Hurley, P. and Duarte, J. P. "Implementation of fiber optic temperature sensors in quenching heat transfer analysis." *Applied Thermal Engineering*, 195, (2021). **Journal Paper**

[12] "LUNA ODiSI 6000 Series Data Sheet," *LUNA Innovations, Tech. Rep.*, (2021). **Technical Specification Sheet**

[13] Figliola, R. S., and Beasley, D. E., Theory and De-sign for Mechanical Measurements, 5 ed. John Wiley and Sons, (2010). **Textbook**